

Preparation and characterization of novel chitosan-based mixed matrix membranes resistant in alkaline media

Leticia García-Cruz,¹ Clara Casado-Coterillo,² Jesús Iniesta,¹ Vicente Montiel,¹ Ángel Irabien²

¹Department of Physical Chemistry and Institute of Electrochemistry, Universidad de Alicante, 03080 Alicante, Spain

²Department of Chemical and Biomolecular Engineering, Universidad de Cantabria, 39005 Santander, Spain

Correspondence to: C. Casado-Coterillo (E-mail: casadoc@unican.es)

ABSTRACT: In this work, mixed matrix membranes (MMMs) based on chitosan (CS) and different fillers (room temperature ionic liquid [emim][OAc] (IL), metallic Sn powder, layered titanosilicate AM-4 and layered stannosilicate UZAR-S3) were prepared by solution casting. The room temperature electrical conductivity and electrochemical response in strong alkaline medium were measured by electrochemical impedance spectroscopy and cyclic voltammetry (CV). The ionic conductivity of pure CS membranes was enhanced, from 0.070 to 0.126 mS cm⁻¹, for the pristine CS and Sn/CS membranes, respectively, as a function of the hydrophilic nature of the membrane and the coordination state of Sn. This hydrophilic and charge nature was corroborated by water uptake measurements, where only the introduction of IL in the CS membrane led to a water uptake of 3.96 wt %, 20 or 30 times lower than the other membranes. Good thermal and chemical stability in alkaline media were observed by thermogravimetric analyses and X-ray photoelectron spectroscopy analyses, respectively, and good interaction between CS and the fillers observed by X-ray diffraction, scanning electron microscopy and CV. Thus, thin CS-based MMMs (40–139 μm), resistant in high alkaline media, show higher conductivity than pure CS membranes, especially those fillers containing tin, and although the electrochemical performance is lower than commercially available anion-exchange membranes they have potential in pervaporation. © 2015 Wiley Periodicals, Inc. *J. Appl. Polym. Sci.* **2015**, *132*, 42240.

KEYWORDS: batteries and fuel cells; composites; electrochemistry; membranes; porous materials

Received 28 November 2014; accepted 19 March 2015

DOI: 10.1002/app.42240

INTRODUCTION

Nowadays, ion-exchange membranes are widely used in the diffusion dialysis, water electrolysis, electrodeionization of aqueous solutions, electrodialysis, electrochemical synthesis for the production of potable and industrial water, for the treatment of industrial effluents and for the chlorine-alkaline production, the demineralization and purification of different products, acid recovery, energy conversion and storage in electrochemical devices.¹ Ion-exchange membranes are usually classified by their function as cation-exchange, anion-exchange and bipolar membranes.² Anion exchange membranes (AEMs) or hydroxide exchange membranes contain fixed positively charged ions and a selective permeation of anions. The general requirements of anion-exchange membranes are low electrical resistance or ionic conductivity of at least 1 mS cm⁻¹, good mechanical and form stability (which means low degree of swelling or shrinking in transition from dry to hydrated state), thermal stability above 100°C, chemical resistance over the entire pH range, and finally, high permselectivity (high permeation to counter-ions and barrier to co-ions).¹

During the last decades, many research groups are focused on production and characterization of AEMs that allow to replace proton exchange membranes (PEMs, usually named Nafion) as electrolyte in order to obtain an improvement of performance in the storage and energy conversion in alkaline electrochemical devices.³ Nafion is a hydrated perfluorosulfonic polymer, in which sulfonate is grafted onto the C-F skeleton of the polytetrafluoroethylene main chains. Although Nafion PEM in fuel cell has experienced a big boom for the last years, there exist persistent problems in terms of permeation crossover, carbonate formation, corrosion, cost and CO poisoning of the costly Pt electrocatalysts.⁴ The main advantages of using AEMs refer to no crossover since the transport is that of anions from anode to cathode and the possibility of using non-precious metals as electrodes.⁵ Moreover, the kinetics of electrochemical processes, such as oxygen reduction, are favored in alkaline media. Commercial AEMs are emerging and being established in the market as proper options and alternatives in alkaline conditions and somewhat overcomes the problems found in based fuel cells using perfluorosulfonic polymers.^{3,6} MEGA and International companies have commercialized strong basic AEMs with good

Table I. Representative Commercial Anion-Exchange Membranes

Membrane	Structure	Applications
FAA 3-PEEK-130 (Fumatech)	Reinforced PEEK (poly ether ether ketone)	Electrodialysis for demineralization, desalination, acid recovery applications, and others
AHA (Astom Corp.)	Polystyrene/Divinylbenzene	Electrodialysis for desalination organic acid recovery and others, diffusion dialysis for acid recovery, membranes for batteries and production of ultrapure water
RALEX® (MEGA):	Quaternary ammonium groups	Electrodialysis, electrodeionization, and electrolysis
AM(H)-PP	Polyethylene/Polypropylene	
AM(H)-PES	Polyethylene/Polyester	
AMI-7001S (International INC.)	Quaternary ammonium groups Polystyrene cross linked with divinylbenzene	Electrodeionization for ultrapure water systems, electrocoating for cathodic and anodic paint systems, electrolysis for biological fuel cells, electrodialysis for desalination and demineralization, and electroplating for metal recovery

thermal and mechanical stability for long periods of time in a pH range 0–14 and 1–11, respectively, in the absence of oxidant species and under frequent regeneration thereof, being the electrolysis and electrodialysis its main applications for which are used. Table I collects the commercial anion-exchange membranes reported so far.

The main drawback is that ionic conductivity is still lower than current PEM. Regarding ionic conductivity, lower resistance and higher stability in high pH medium, the best AEMs are FAA (Fumatech, Germany) and AHA (Astom Corp., Japan), also seen in Table I. The former is being widely employed as polymer electrolyte for direct alcohol fuel cell because of its conductivity around 8 mS cm^{-1} and electrical resistance below $2 \Omega \text{ cm}^{-2}$. However, these commercial membranes are generally based on divinylbenzene which increases greatly the cost, as well as cross-linked polystyrene and aminated cross-linked polystyrene, which limit the chemical and thermal stability at high pH and temperature. Besides the low anion conductivity as well as carbonation are still challenges to be faced. Commercial AEMs are also usually rather thick in order to avoid crossover of fuels (H_2 , O_2 , or alcohols) in fuel cells and water electrolysis applications.⁷ Several strategies have been attempted to improve membrane properties by altering the chemistry of the polymer,⁴ or hybridizing via sol-gel methods to introduce inorganic components in the polymer matrix.⁸ Even though the performance of a membrane with good electrical conductivity and good thermal and mechanical stability is of great interest, the need for cheap, biocompatible and eco-friendly materials, is increasingly demanded to avoid the use of dangerous preparation methods and toxic chloromethyl compounds.

In this regard, chitosan (CS), a derivative from chitin, is a low-cost, biocompatible, and weak cationic polyelectrolyte (with a pK_a of ca. 6.5), obtained from natural resources,⁹ containing functionalized groups that allow tuning the ionic character. In

the dry state, an unmodified CS membrane is very fragile, and non-conductive.¹⁰ Upon water swelling, the ionic conductivity of the CS membrane has been reported as remarkable.¹¹ However, the use of unmodified CS membranes in fuel cell configuration is limited by the robustness and low ionic conductivity even at hydrated CS membranes.¹⁰

The first approach of the preparation of solid polyelectrolyte membranes based on CS was focused on the CS–salt complex using potassium hydroxide as binder between two CS layers,¹² providing an ionic conductivity of $1 \times 10^{-2} \text{ S cm}^{-1}$ after hydration. The second approach was focused on the use of organic–inorganic hybrid membranes, that is, the use of several inorganic blocks have been used in the literature for the improvement of the mechanical and physical stability of the material.¹³ Mixed matrix membranes (MMMs), consisting of the combination of a continuous polymer matrix with a small amount of dispersed fillers, either organic or inorganic, as a means of obtaining an heterogeneous membrane with synergistic properties of the fillers (conductivity, flexibility, or molecular sieving) and the polymer (low cost and processability) may improve the thermal, mechanical, and electrical properties of CS membranes for their use in fuel cells.¹⁴ Polyvinyl alcohol membranes have been modified by titanium oxide nanoparticles,¹⁵ and clays.¹⁶ Likewise, quaternary CS membranes were modified by alkoxysilane-containing positively charged precursors by sol-gel methodology in order to create hybrid covalently SiO_2 -CS nanocomposites¹⁷ with an ionic conductivity of $1.89 \times 10^{-2} \text{ S cm}^{-1}$ at 80°C . The incorporation of microporous ETS-10 titanasilicate into CS has been seen to improve the performance of the pure polymer in the pervaporation separation of water/ethanol mixtures.¹⁸ Layered inorganic materials such as clays have been used to improve CS and other natural polymers mechanical and thermal resistance.¹⁹ Other alternatives have come out recently like cellulose acetate-CS blends²⁰ or the use of room temperature ionic liquids (RTILs)²¹ for application as

polymer electrolyte membranes. The incorporation of inorganic blocks to pristine CS membranes generally contributes to enhance the mechanical and physical stability of the material in addition to decrease the water uptake and the permeability of small alcohol molecules.²²

Thus, the aim of the article is to study the feasibility of novel membrane materials based on green chemistry as alternative materials in electroanalyses, organic electrosyntheses,²³ and fuel cell technology, namely, CS-based MMMs prepared using several fillers as proof of concept in the MMM approach. These fillers are: layered nanoporous materials prepared without organic surfactants, such as AM-4 titanosilicate,²⁴ and novel stannosilicate, UZAR-S3,²⁵ with Sn isomorphously substituted in the silicate framework, tin metallic nanoparticles,²⁶ and 1-Ethyl-3-methylimidazolium acetate ionic liquid (IL) as an example of the effect of the cation–anion tuneability of RTILs as well as the interaction between polysaccharides and ionic liquids as a way to control the rigidity of semicrystalline CS structures.²⁷ Results and discussion will be provided in terms of the electrochemical characterization by cyclic voltammetry (CV) and electrochemical impedance spectroscopy (EIS) to assess the ionic conductivity of the new membranes. Other physicochemical characterization [scanning electron microscopy (SEM), X-ray diffraction (XRD), thermogravimetric analysis (TGA), and water uptake] are also discussed.

EXPERIMENTAL

Membrane Preparation

CS (coarse ground flakes and powder, Sigma-Aldrich) with molecular weight from 310,000 to > 375,000 and 75% deacetylation degree, based on the viscosity range of 800–2000 mPa s, was used as purchased. CS membranes and MMMs were prepared according to previously reported procedures.^{18,26} In a typical synthesis, CS powder was added to the acetic acid/water mixture and stirred at room temperature for 24 h. A transparent, viscous and homogeneous solution of 1 wt % CS was obtained. Then 10 mL of CS solution were degassed in an ultrasound bath for 5 min and cast on a polystyrene Petri dish. Evaporation to constant weight takes 2–3 days before the membrane can be peeled off the Petri dish. Thicknesses were measured with a Mitutoyo digital micrometer (Japan), in at least 4–5 spots over the membrane area. The weight of the dried membranes was also measured at this point in an electronic balance to calculate the density of the membranes.

MMM were prepared by dispersing a certain amount of inorganic filler in the solvent before adding to the CS solution in order to obtain a 20 wt % filler: CS ratio. Then, the mixture was stirred until homogeneity. This mixture was degassed in an ultrasound cleaning bath for 10 min and cast in the same way as pure CS membranes.

The fillers used for the synthesis of CS-based MMMs were microporous lamellar titanosilicate AM-4 ($\text{Na}_3(\text{Na}, \text{H})\text{TiO}_2(\text{Si}_2\text{O}_6)_2 \cdot 2\text{H}_2\text{O}$) synthesized as in Casado *et al.*,²⁴ a layered stannosilicate UZAR-S3 ($\text{Na}_7\text{Sn}_2\text{Si}_9\text{O}_{25}$).²⁵ They are composed of Ti and Sn pyramid layers separated by galleries containing Na^+ cations accounting for high ion-exchange capacity.²⁸ These

layers can be exfoliated after protonation in the acetic acid aqueous solution where CS is dissolved. Sn powder (150 nm, 2100 mesh, 99.5%, Alfa Aesar) was dispersed in the CS 1 wt % solution after dispersion in 2 wt % acetic acid/water. Regarding the incorporation of [emim][OAc] ionic liquid (IL) (assay $\geq 96.5\%$, Aldrich), this was added directly to the stirring CS solution in a 5 wt % proportion to the CS content in the final membrane.

Physicochemical Characterization of the Membranes

The morphology of the CS and MMMs was observed by SEM and was performed on the surface and cross-section of the samples using a Zeiss DMS 942 instrument operating at 30 kV.

X-ray photoelectron spectroscopy (XPS) experiments were recorded on a K-Alpha Thermo Scientific spectrometer using $\text{AlK}\alpha$ (1486.6 eV) radiation, monochromatized by a twin crystal monochromator and yielding a focused X-ray spot with a diameter of 400 μm , at 3 mA \times 12 kV. Deconvolution of the XPS spectra was carried out using a Shirley background.

The XRD patterns of the membranes were collected on a Philips X'Pert PRO MPD diffractometer operating at 45 kV and 40 mA, equipped with a germanium Johansson monochromator that provides $\text{Cu K}\alpha_1$ radiation ($\lambda = 1.5406 \text{ \AA}$), and a PIXcel solid angle detector, at a step of 0.05° .

The thermal stability of the samples was studied by thermogravimetric analyses (DTA-TGA) using a thermo balance (DTG-60H, Shimadzu, Japan) in air at heating rate of $10^\circ\text{C min}^{-1}$ up to 700°C . Samples of approximately 2–5 mg were loaded into an alumina crucible and a reference pan was left empty during the experiment.

Water uptake of CS-based membranes was estimated by measuring the change in weight of the membrane before and after hydration, that is, the process of adsorption of large quantities of water molecules by the membrane material, which resulted on a swelled membrane with a considerable increase in volume. The OH^- form of the membrane was immersed in deionized water at room temperature and equilibrated for 24 h. The wet weight of the membrane, W_{wet} , is determined by quickly removing the excess water and weighing in a precision balance. The percentage of water content is calculated using eq. (1)

$$W(\%) = \left(\frac{W_{\text{wet}} - W_{\text{dry}}}{W_{\text{dry}}} \right) \times 100 \quad (1)$$

where W_{dry} is the weight of the dried membrane after removal from the Petri dish.

The electrochemical characterization of the unmodified CS membrane and CS-based MMMs was carried out in a three-electrode configuration glass cell, using a glassy carbon electrode (GCE) of 3.0 mm diameter (Good Fellow Inc., UK). The membranes are placed and adhered firmly onto the glassy carbon surface. A gold wire was used as counter electrode and an Ag/AgCl (3.5M KCl) as reference electrode.

GCE substrates were eroded using alumina powder and water as lubricant (1.0, 0.3, and 0.05 μm particle size, respectively) for 4 min each. Thereafter, the GC was sonicated under an ultrasonic

cleaning bath for 1 min and dried under argon atmosphere. CS-based MMMs, supported onto the GCE were equilibrated in a 1M NaOH aqueous solution at a controlled potential of -0.25 V versus Ag/AgCl (3.5M KCl) for 15 min. Thereafter, the CV of the membrane/GCE anode was recorded between -0.25 and $+0.15$ V at 50 mV s^{-1} . CV measurements were performed at 293 ± 2 K under Ar atmosphere, using an Autolab III potentiostat/galvanostat (Eco-Chemie).

The electrochemical impedance spectroscopy (EIS) measurements were carried out in order to obtain the specific conductivity of all membranes synthesized in this work. EIS experiments were performed using a microAutolab equipped with a FRA impedance module at open circuit potential (potentiostatic method). The pristine CS membrane and the CS-based MMMs were placed between stainless steel-plated electrodes with a geometric area of 1.13 cm^2 and the EIS cell was subjected to a constant pressure until the Nyquist plot of the EIS response was repeatedly the same. The amplitude was set at 10 mV and the frequency range was varied between 1 MHz and 100 Hz. The EIS experiments were performed at controlled temperature of 295 ± 3 K. Before EIS experiments, membranes were reactivated in 1M NaOH for 24 h and rinsed with ultrapure water. Finally, water was removed from the membrane surface using a dried paper before placing it in the EIS cell. For calculating the ionic conductivity of CS membranes a stack method was employed, which consisted of measuring the impedance spectroscopy of one, two, and three membranes stacked together in the EIS cell, respectively. From the slope of resistance versus thickness plot, the conductivity of each MMM can be calculated.^{29,30}

RESULTS AND DISCUSSION

Structural Characterization

The morphology of the CS-based MMMs can be observed in the SEM images of CS, IL/CS, AM-4/CS, UZAR-S3/CS, and Sn/CS MMMs in Figure 1. Pristine CS and IL/CS membranes [Figure 1(A,B)] reveal a flat surface so the incorporation of a 5 wt % of the IL into the pristine CS membrane had no effect on the morphology of the IL/CS membrane, which shows a continuous matrix. The incorporation of layered titanosilicate AM-4 into the CS matrix leads to a heterogeneous, rough surface, whereas after the incorporation of lamellar stannosilicate UZAR-S3, a more compact and homogeneous surface is observed [Figure 1(C,D)]. However, it can be noted from the cross sections of AM-4/CS and UZAR-S3/CS MMMs that AM-4 particles were distributed homogeneously throughout the membrane thickness, while UZAR-S3 was found only on the surface of the membrane. Figure 1(E) corresponds to the Sn/CS membrane with a 20 wt % metallic Sn loading, where the particle size was checked to belong in the micrometer range and well dispersed throughout the polymer matrix. These cross-section images reveal thus the anisotropy of the distribution of the inorganic fillers (tin, layered porous titanosilicate and stannosilicate) in the CS polymer matrix. The horizontal orientation of microporous layers in the CS matrix could control the ion transport and conductivity across the membrane in comparison with the neat polymer.³⁰

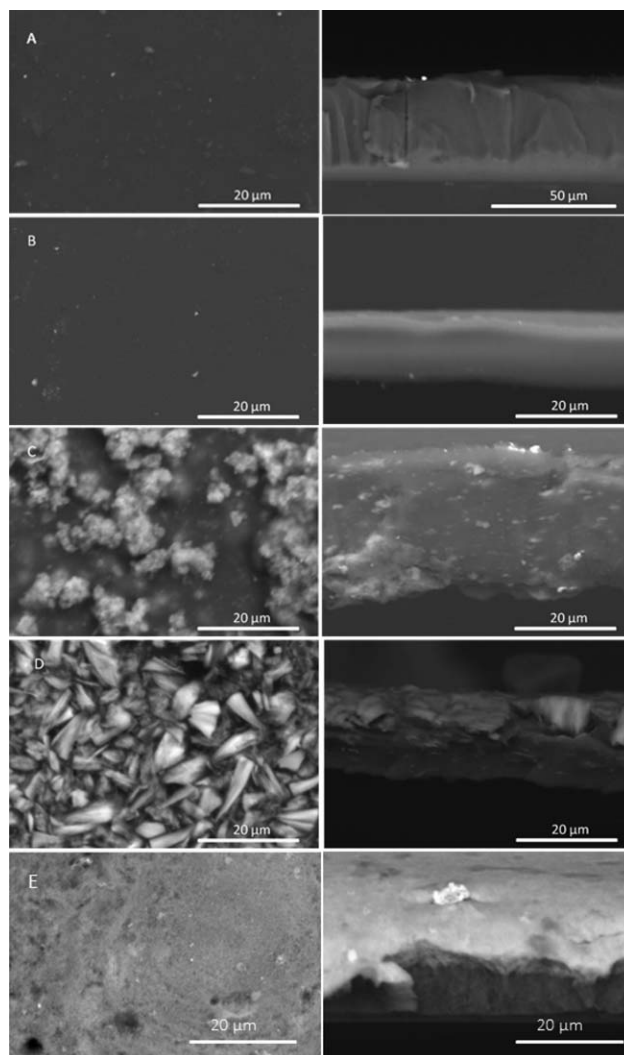


Figure 1. SEM photographs of the CS-based MMMs: (A) CS, (B) IL/CS, (C) AM-4/CS, (D) UZAR-S3/CS, and (E) Sn/CS membranes. The figures represent the surface (left column) and cross-sectional (right column) view of the membranes.

The XRD patterns of the CS pure and hybrid membranes are shown in Figure 2. The CS membranes exhibit the semicrystalline nature by characteristic of the crystalline forms of CS: form I at $2\theta = 11.2$ and 18.0° and form II at 20.9 and 23.8° ,¹⁸ for the hydrogen bonds and hydroxyl and amino groups on the CS chains. The crystalline domain is completely destroyed after adding the 5 wt % IL. After incorporation of the layered compounds AM-4 and UZAR-S3, a band appears at low angles, characteristic of the d -spacing between the crystalline nanoporous layers.^{24,25} This band is more remarkable in the latter case, since the exfoliation of the former, AM-4 titanosilicate, is particularly difficult,²⁴ and swollen layers are mostly deposited onto CS matrix surface as shown in SEM images [Figure 1(D)]. In the XRD pattern of the Sn/CS MMM, the reflections of tin are observed (marked by asterisk in Figure 2), as compared with the data from JCPDS–International Centre for Diffraction Data. It can also be observed that the CS broad peaks are

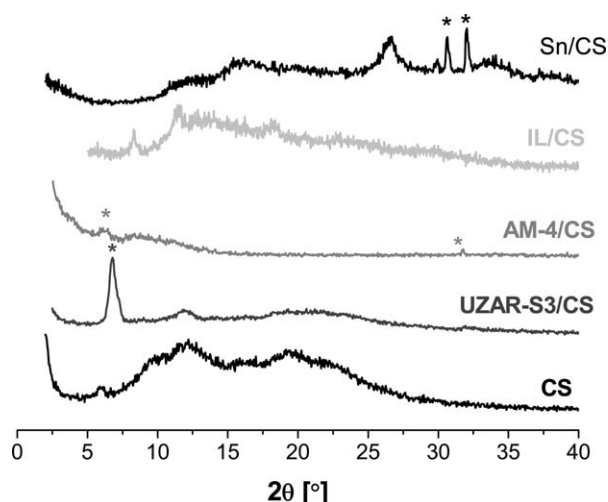


Figure 2. XRD patterns of (from bottom to top) CS membrane, UZAR-S3/CS, AM-4/CS, IL/CS, and Sn/CS MMMs samples in the OH^- form.

reduced upon addition of inorganic fillers and this is attributed by changes in the ordering of the chain packing and interaction between the components of the membrane.³¹ Generally, the incorporation of inorganic fillers alters significantly the crystallinity of the membrane and therefore the crossover of hydroxide ions is higher in the swollen membrane with an increase in ionic conductivity.¹⁴

XPS was performed on the AM-4/CS, UZAR-S3/CS, and Sn/CS MMMs where deconvolution of the XP spectra (Table II) revealed that the analysis of 1s binding energies, atomic fractions and assignments for the elements of C, O, and N are consistent with the values found in literature for pristine CS.^{32,33} According to XPS data shown in Table II, the 1s binding energies of the elements C, O, and N for the membranes with different inorganic fillers reveal no significant differences—within an error of 0.5 eV—thereby XP spectra probes clearly that neither hydroxyl nor amino groups in the CS matrix are involved in any chemisorption process with the inorganic fillers AM-4, UZAR-S3, and Sn nanoparticles. All XP spectra showed only one peak at N 1s (399.9 eV) denoting the presence of $-\text{NH}_2$ or $-\text{NH}-$ groups of CS,³⁴ and suggesting no complexation of the N atom by the heteroatoms from the inorganic fillers, which agrees with the expectation that crosslinking reactions only occurred at R-NH_2 and thus the ion transport would not substantially change across the membranes because of the weak basic properties of the amino groups in the CS compared with the alkaline fillers.³⁵

The presence of Sn nanoparticles is observed by XPS for the Sn/CS membrane, with a binding energy of 486.8 eV for the Sn $3d^{5/2}$. Moreover, the XP spectrum also confirms the presence of TiO_2 and SiO_2 in the titanosilicate in AM-4/CS MMM by binding energies of 458.56 eV for Ti $2p^{3/2}$ and 102.25 eV for the Si $2p^{3/2}$. Similar observation regarding the presence of SiO_2 and SnO of the stannosilicate in UZAR-S3/CS MMMs, by the binding energies 102.51 eV for Si $2p^{3/2}$, and 486.97 eV for Sn $3d^{5/2}$.

Table II. Deconvolution of the XPS Spectra Obtained for the Sn/CS, UZAR-S3, and AM-4/CS MMMs, and the Assignments Based on the Binding Energies

Element	Sn/CS	UZAR-S3/CS	AM-4/CS	Assignment
C 1s	285.01 (31.76)	285.02 (28.42)	285.11 (22.80)	C—C and $\text{Csp}^3\text{—H}$
C 1s	286.58 (22.53)	286.54 (22.30)	286.58 (22.51)	C—O or C—N or C—O—C
C 1s	287.99 (11.86)	287.94 (13.46)	288.03 (12.89)	C=O or O—C—O
O 1s	531.4 (5.22)	531.37 (3.85)	531.67 (5.55)	C=O or C—O—C or hydroxide
O 1s	532.92 (21.23)	532.85 (22.59)	532.96 (20.13)	>C—O or OH or bound H_2O
O 1s	—	—	530.15 (5.16)	TiO_2
N 1s	400.0 (6.69)	399.9 (7.11)	400.07 (6.82)	$-\text{NH}_2$ or $\text{NH}-$
Si $2p^{3/2}$	—	102.51 (1.41)	102.25 (1.63)	SiO_2
Ti $2p^{3/2}$	—	—	458.56 (1.9)	TiO_2
Sn $3d^{5/2}$	486.8 (0.71)	486.97 (0.19)	—	SnO_2

Atomic weight percentage values are presented between brackets.

Table III. Composition of CS-based Membranes, Thickness, Density, Water Uptake, Thermal Degradation Temperature, and Ionic Conductivity of CS, IL/CS, AM-4/CS, UZAR-S3, and Sn/CS Membranes

Membrane	Thickness (μm)	Density (g cm^{-3})	W_u (wt %)	$T_{d,\text{OH}}$ ($^{\circ}\text{C}$)	Conductivity ^a (mS cm^{-1})
CS	41.0 ± 11	1.076 ± 0.46	124 ± 2.5	228	0.070
IL/CS	87.8 ± 13	1.175 ± 0.39	3.96 ± 1.9	142	0.098
AM-4/CS	82.2 ± 4.0	0.536 ± 0.16	98.5 ± 9.2	176	0.082
UZAR-S3/CS	139 ± 4.7	0.803 ± 0.36	100 ± 16	258	0.070
Sn/CS	70.0 ± 9.7	1.128 ± 0.52	126 ± 14	229	0.126
FAA-PEEK-130 (Fumatech, Germany)	130	1.178^b	24.1^b	N.A.	2.92
AHA (Astom Corp., Japan)	220	0.830^b	22.8^b	N.A.	3.22

The properties of FAA and AHA commercial membranes measured in the same conditions are also shown for comparison.

^aConductivity calculated using the method of a stack of three membranes by impedance spectroscopy technique, after activation in 1 M NaOH for 24 h.

^bMeasured in the laboratory.

The peak corresponding to TiO_2 appearing at 458.56 eV in UZAR-S3/CS, is moved to 532.96 eV in AM-4/CS, where the O 1s is more remarkable. This agrees with the presence of the titanosilicate all over the membrane matrix observed by SEM, where the stannosilicate stays mainly on the surface. The atomic weight percentages also shown in Table II indicate the embedding of the particles within the CS matrix. Ti, Si, Sn contents agree with the elementary composition of the inorganic fillers employed.^{24,25} Furthermore, interestingly there is a visible decrease in C-C or C sp^3 -H moieties of the deconvoluted C 1s core element; 22.80%, 28.42%, and 31.76%, for AM-4/CS, UZAR-S3/CS, and Sn/CS MMMs, respectively. These differences can be ascribed to possible surface contamination and the presence of residual acetate groups adsorbed in the CS membrane during the synthesis,³³ probably due to incomplete ion exchange upon neutralization.

The thickness was measured and used to calculate the apparent density as well as the conductivity of the membranes. Both values influence the free volume and transport of species across the membranes. The density values of the IL/CS and Sn/CS membranes do not differ much from pristine CS, as shown in Table III. The observed differences in density when the filler is a layered porous material could be related to the increase of free volume by the disruption caused by the layered barriers between the polymer chains. Free volume is directly related to the diffusion properties across the membrane. This effect is more remarkable for AM-4 than UZAR-S3, since the former is distributed within the whole matrix and the latter only in the surface, as observed by SEM in Figure 1(C,D).

The thermal stability of the membranes is a key parameter to guarantee the functionality of these membranes in different environments at various temperatures for a long term. Thermal degradation of CS and CS-based MMMs was examined in the range 25–700 $^{\circ}\text{C}$ and the TGA-DTA curves are represented in Figure 3. The degradation of CS involves the usual three stages: a first stage up to 100 $^{\circ}\text{C}$ for the evaporation of the free water adsorbed in the membrane, a second stage from 150 to 350 $^{\circ}\text{C}$

for the removal of bound water and start of deacetylation and depolymerization of CS and a third stage for the residual decomposition of the main polymer (350–700 $^{\circ}\text{C}$). The weight loss observed below 100 $^{\circ}\text{C}$ is thus attributed to the water present as free water in the CS matrix, which is responsible to the ion migration through the membrane material.³⁶ The second stage is the one identifying the thermal stability of the membranes, from where the degradation temperature has been extracted as the temperature at which 5 wt % of weight is lost, once free water has been removed given the high hydrophilicity of the OH^- form of the membranes.³⁶ The thermal degradation temperature thus calculated (Table III) is higher for the inorganic layered particles-filled MMMs than for the pristine CS membrane. Sn/CS MMMs show the same degradation temperature as the pure polymer. This can be explained by the residual weight observed in Figure 3, which gives a real loading of 11, 17, and 15 wt % for Sn, UZAR-S3, and AM-4 in the MMM, respectively, which is lower than the nominal 20 wt % loading expected. Since the thermograms were measured from the

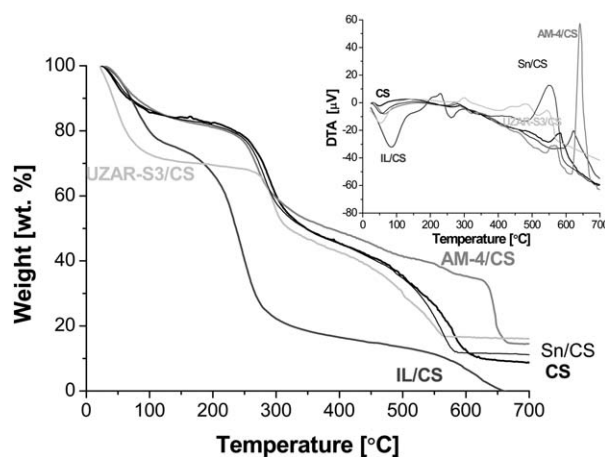


Figure 3. Thermal analysis of CS-based membranes. Inset: DTA curves of the membranes.

membranes in OH^- form, these differences may be attributed to the morphology observed by SEM, since all the MMMs present accumulation of particles on their surface, or migration of excess of particles to the NaOH neutralization solution. This agrees with the higher homogeneous dispersion of AM-4 throughout the whole polymer matrix, and not only along the surface, as the other inorganic fillers.

The water content of the anion-exchange membranes is thus a crucial parameter in fuel cell technology because the conductivity of OH^- membranes usually increases significantly when hydrated. In general, a high degree of hydration is related to lower thermal degradation temperature, and it also depends on the chemical nature and composition of the membrane materials. Table III collects the data on the water uptake and degradation temperature for the CS-based MMMs. The water uptake of pristine CS membranes is 124%, which is quite high but lower than that reported for CS-based MMMs.²⁷ This value decreases slightly up to around 100% for the MMMs prepared with the layered silicate precursors, AM-4 and UZAR-S3, while it is not affected by the addition of Sn particles, and this agrees with the thermal degradation of the OH-form membranes. Therefore, it can be attributed to the hydrophilicity of metallic tin compared with its coordinated form in a silicate framework.³⁷ On the other hand, the presence of IL reduces significantly the water uptake mainly due to the interactions inside the membrane between the amino and hydroxyl groups of CS matrix and the acetate anion and imidazolium cation of the IL, which reduces the solvation of CS by the water between the chains by the additional presence of IL.²⁹ The enhancement of the hydrophobicity of the membrane by IL could be a plausible reason for the prevention of entering water and swelling of the IL/CS membrane. Water content in CS is present as free and bound water and only the former is deemed responsible for the anion conductivity.³⁸ The free water content is calculated from the difference between the weight loss at 100°C and at the first onset in the DTA curves on the inset in Figure 3, and it is the lowest for the IL/CS membranes (5 wt %). On the other hand, the SEM observations in Figure 1 assure that the layered inorganic fillers AM-4 and UZAR-S3, as well as the Sn particles, are really dispersed in the matrix and were not washed away during synthesis. The excessive water uptake may contribute to loss of mechanical and morphological stability of the membranes, thus a compromise is usually necessary given the importance to the electrochemical performance of the membrane.³⁹ The introduction of IL in CS membranes has been observed to reduce the mechanical strength and largely increase the flexibility of the chains and the introduction of titanosilicates can increase both properties, compared with the pristine CS membrane.²⁷

CV Measurements

Figure 4 shows the CV behavior conducted for pristine CS and CS-based MMM materials onto a GCE bar electrode. The cyclic voltograms at bare GCEs are also represented in order to compare the capacitive current with and without modification. The coating of the GCE substrate with a 41 μm -thick CS membrane leads to a considerable increase in capacitive current compared with the unmodified GCE. These results show that the electroactive area of the CS-modified-GCE increases due to the

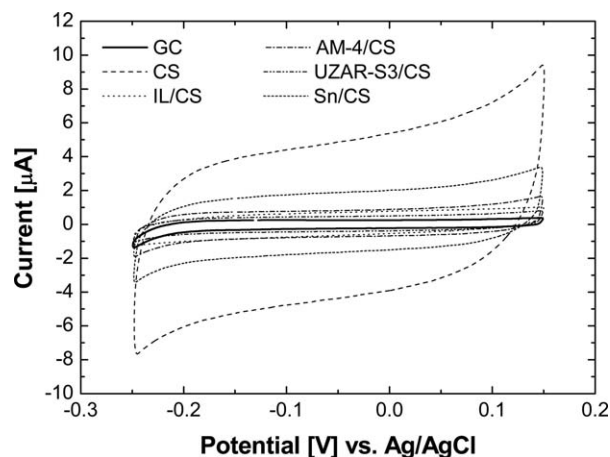


Figure 4. Electrochemical behavior of the CS-based membranes in 1M NaOH. Scan rate 50 mV s^{-1} . The fifth scan is recorded.

reactive amino and hydroxyl groups present in the CS structure. A similar behavior was observed by Fatibello-Filho's group,⁴⁰ where a CS film supported on a graphite-epoxy electrode revealed a high capacitive current compared to the unmodified electrode.

In this work, hybridization of CS by the introduction of IL, AM-4, UZAR-S3, and Sn fillers, in this order, results in a decrease of this capacitive current. The loss of the electroactive area is presumably due to the interaction between the fillers (IL, layered porous materials, AM-4 and UZAR-S3, and Sn particles) and the hydroxyl groups of the CS matrix.³⁰ An additional reason can be that the CV response of the MMMs may be affected by the water uptake of the membrane. The results given in Table II indicate that the water uptake is slightly larger for CS and Sn/CS membranes than for the IL/CS, AM-4/CS, and UZAR-S3/CS membranes. A high relative water uptake of the membrane will allow ions to go through the membrane, which results in an increase in capacitive current. Therefore, the layered silicates decrease the water uptake and electroactive area, diminishing the capacitive current as a consequence of the barrier effect and anisotropy introduced by the nanoporous layers in the polymer matrix.³⁰

Impedance Electrochemical Spectroscopy Measurements

Electrochemical impedance spectroscopy provided typical plots of Nyquist curves for MMMs, as shown in Figure 5. To extract the through-plane membrane resistance from the Nyquist plot, the membrane resistance is determined by extrapolating the linear portion of the low frequency part of the Nyquist plot to the real part axis (x -axis).⁴¹ The typical equivalent circuit used for the determination of the membrane conductivity is depicted in Scheme 1,⁴² where W is the Warburg element or diffusive element; R_{hf} is the resistance at high frequency which corresponds to the combination of internal resistance R_{int} (the resistance between the electrode and membrane surfaces namely also the free water surface), the electrode resistance, R_{elec} , and the bulk membrane resistance, R_{mem} , that is, the resistance of polymeric membrane, which is the major contributor in R_{hf} .⁴³ Finally, R_p denotes the polarization resistance or the charge transfer resistance and CPE is the constant phase element. CPE is due to a

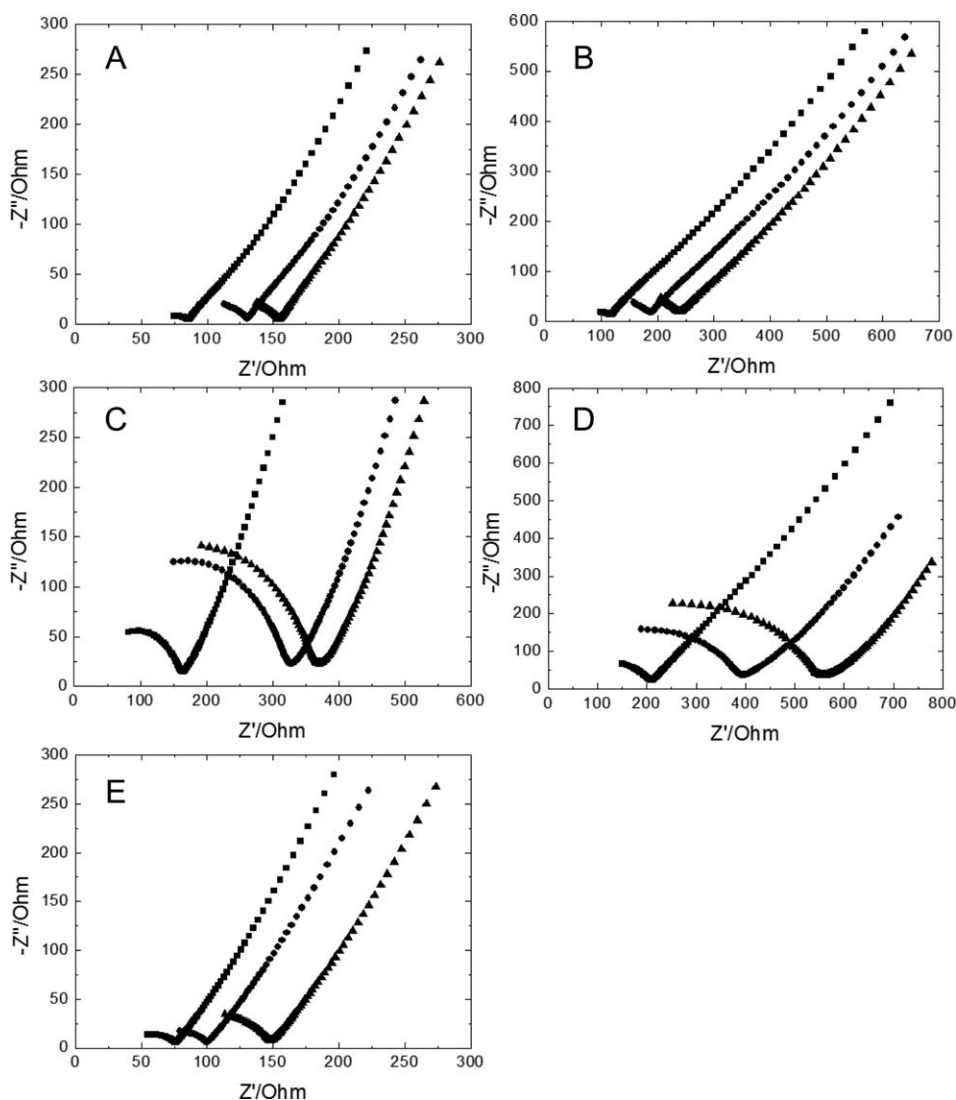


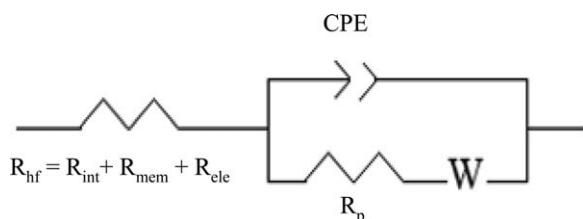
Figure 5. Nyquist plots show the impedance response of CS (A), 5 wt % IL/CS (B), 20 wt % AM-4/CS (C), 20 wt % UZAR-S3/CS (D), and 20 wt % Sn/CS (E) MMMs at room temperature (100 Hz - 1 MHz, open circuit potential). ■ Single membrane, ● two membrane stack, and ▲ three membrane stack.

surface non-homogeneity that provides a non-uniform distribution of current density over the electrode.⁴¹

According to Figure 5, the Nyquist plot is very dependent on the type of filler used for the modification of the pristine CS, though in all cases, the spectra obtained include a linear region at low frequencies related to diffusion control.³⁰ The diameter of the kinetic loop increases for AM-4/CS, UZAR-S3/CS MMMs

and more slightly for the Sn/CS MMM. When the nanoporous layers inorganic fillers are incorporated in the polymer matrix of pure CS, the polymer area or electroactive area is changed and its porosity is also modified, it is increased, as shown in SEM images. The modified matrix and higher porosity can produce an increment of resistance within the polymeric matrix and, therefore, an increment of semicircle diameter associated with higher frequencies. As far the IL/CS membranes behavior is concerned, the semicircle is similar to pristine CS, suggesting that the surface of the polymeric matrix is slightly modified when the IL is incorporated into the polymeric matrix.

The ionic conductivity of the MMMs is obtained from the Nyquist plots represented in Figure 5. The ionic conductivity values of the novel membranes prepared in this work are shown in Table II. CS membrane shows a specific conductivity 0.070 mS cm^{-1} , which agrees with other CS membranes reported in the literature, where theoretical ionic conductivity values of



Scheme 1. Equivalent electrical circuit used to fit the impedance spectra.

0.123 mS cm⁻¹ at 25°C⁴⁴ and experimental ionic conductivities of about 0.1 mS cm⁻¹^{10,11,45} are given. In this work, the incorporation of IL, AM-4, UZAR-S3 or Sn, increased the specific conductivity of pristine CS membranes. The ionic conductivity of [CBIM]I ionic liquid-CS composite membranes has been reported as high as 9.1 mS cm⁻¹ measured in N₂ atmosphere and room temperature, but at a IL: CS ratio as high as 140 wt %, ⁴⁶ when our IL : CS ratio is only 5 wt % to have a solid dense membrane. However, the ionic conductivity of IL/CS composites has also been reported to increase from 9.86 × 10⁻⁶ S cm⁻¹ to 2.60 × 10⁻⁴ S cm⁻¹ with increasing doping IL from 10 to 150 wt % due to the aggregation of charge carriers.⁴⁷ In any event, the ionic conductivity of the membranes developed in this work is still lower than those values obtained for the commercial AEMs, FAA-3-PK-130 (7.6 mS cm⁻¹, Fumatech, Germany) and AHA (4.9 mS cm⁻¹, Astom, Japan)⁴⁸ that give values of 2.92 and 3.22 mS cm⁻¹, respectively, under the same experimental conditions as the CS-based membranes.

The advantages of the membranes prepared in this work are their thermal stability, thicknesses three times lower than the commercial membranes and the fact that they are prepared from eco-friendly and economic materials containing functional groups, which make unnecessary the use of additional ammonium quaternary groups that are not so stable at high pH values and elevated temperatures, as the commercial AEMs. The ionic conductivity of our home-made CS composite membranes is still two orders of magnitude lower than the ionic conductivity of the commercial AEMs. The present work is a preliminary study on the preparation and characterization of novel CS-based membranes and their potential use in electrochemical devices, if the ionic conductivity reached the standards in AEMs. Regarding the membranes presented in this work, since the ionic conductivity values are lower than those of commercial AEMs, restricting their use in electrochemical devices, these membranes have been proved useful in pervaporation.⁴⁹

CONCLUSIONS

The main properties of anion-exchange membranes (AEMs) are high anion conductivity, resistance in alkaline media, thermal and mechanical stability, and low permeability. In this work, MMMs were prepared by solution casting from CS biopolymer, as continuous matrix, and a non-toxic ionic liquid, tin particles, layered titanosilicate AM-4 and stannosilicate UZAR-S3 particles, as fillers. The MMMs thus obtained were characterized by SEM, XRD, TGA and XPS. In order to evaluate their potential use as AEMs in electrochemical processes, the ionic conductivity was measured by EIS and compared with commercially existing membranes. All the MMMs showed a rather homogenous dispersion of the fillers upon the membrane matrix except UZAR-S3, which stood at the surface of the membrane, as observed by SEM. The XRD revealed the presence of the tin particles in the Sn/CS membrane as well as a partial exfoliation in the AM-4/CS membrane, more pronounced in the UZAR-S3/CS MMM, because of the thinner nature of the layers of the stannosilicate. The introduction of IL in the CS matrix decreased the crystallinity of pristine CS membrane and the water uptake and swelling as measured by TGA. Thermal analyses also revealed two

different kinds of water in the CS-based MMMs, and a thermal stability up to 200°C, for the inorganic-filled MMM, which diminished for the IL/CS MMM. XPS revealed that crosslinking of CS with the inorganic fillers occurred mainly with the amino groups in the CS matrix, thus only OH⁻ ions are available for ion transport. The thicknesses of the MMMs were in the range 40–139 μm, thus generally lower than those of commercial AEMs. The CV revealed resistance in high alkaline media, but, finally, the ionic conductivity, though increased compared to pure CS membranes (0.070 mS cm⁻¹), especially those with fillers containing tin (0.126 mS cm⁻¹), was still much lower than that of commercial AEMs. Although this is the first work studying the conductivity of CS-based MMMs their use as alternative AEMs in electrochemical devices is still not possible, however, they did show advantages in other membrane separations, such as pervaporation.

ACKNOWLEDGMENTS

This work has been funded by the Spanish MINECO through grants CTQ2010-20347, at the University of Alicante, and CTQ2012-31229 and RYC2011-08550, at the University of Cantabria. The authors gratefully thank Prof. Frank Marken, from the University of Bath (UK), for his advice on the electrochemical impedance characterization, and Dr. César Rubio, Dr. Carlos Téllez, and Prof. Joaquín Coronas, from the University of Zaragoza and the Instituto de Nanociencia de Aragón, Spain, for the UZAR-S3 sample and fruitful discussions.

REFERENCES

1. Strathmann, H.; Grabowski, A.; Eigenberger, G. *Ind. Eng. Chem. Res.* **2013**, *52*, 10364.
2. Xu, T. *J. Membr. Sci.* **2005**, *263*, 1.
3. Merle, G.; Wessling, M.; Nijmeijer, K. *J. Membr. Sci.* **2011**, *377*, 1.
4. Huang, A.; Xia, C.; Xiao, C.; Zhuang, L. *J. Appl. Polym. Sci.* **2006**, *100*, 2248.
5. Antolini, E.; Gonzalez, E. R. *J. Power Sources* **2010**, *195*, 3431.
6. Couture, G.; Alaaeddine, A.; Boschet, F.; Ameduri, B. *Prog. Polym. Sci.* **2011**, *36*, 1521.
7. Carmo, M.; Fritz, D. L.; Mergeand, J.; Stolten, D. *Int. J. Hydrogen Energy* **2013**, *38*, 4901.
8. Wu, C.; Wu, Y.; Xu, T.; Fu, Y. *J. Appl. Polym. Sci.* **2008**, *107*, 1865.
9. Krajewska, B. *J. Chem. Technol. Biotechnol.* **2001**, *76*, 636.
10. Wan, Y.; Creber, K. A. M.; Peppley, B.; Bui, V. T. *Polymer* **2003**, *44*, 1057.
11. Wan, Y.; Creber, K. A. M.; Peppley, B.; Bui, V. T. *J. Membr. Sci.* **2006**, *280*, 666.
12. Wan, Y.; Creber, K. A. M.; Peppley, B.; Bui, V. T.; Halliop, E. *Polym. Int.* **2005**, *54*, 5.
13. Kickelbick, G. *Prog. Polym. Sci.* **2003**, *28*, 83.
14. Ma, J.; Sahai, Y. *Carbohydr. Polym.* **2013**, *92*, 955.

15. Yang, C.-C.; Chien, W.-C.; Li, Y. J. *J. Power Sources* **2010**, *195*, 3407.
16. Yang, C.-C.; Lee, Y.-J.; Chiu, S.-J.; Lee, K.-T.; Chien, W.-C.; Lin, C.-T.; Huang, C.-A. *J. Appl. Electrochem.* **2008**, *38*, 1329.
17. Wang, J.; Wang, L. *Sol. State Ionics* **2014**, *255*, 96.
18. Casado-Coterillo, C.; Andrés, F.; Téllez, C.; Coronas, J.; Irabien, A. *Sep. Sci. Technol.* **2014**, *49*, 1903.
19. Zuo, G.; Wan, Y.; Wang, L.; Liu, C.; He, F.; Luo, H. *Mater. Lett.* **2010**, *64*, 2126.
20. Xiao, W.; Wu, T.; Peng, J.; Bai, Y.; Li, J.; Lai, G.; Wu, Y.; Dai, L. *J. Appl. Polym. Sci.* **2013**, *128*, 1193.
21. Xiong, Y.; Wang, H.; Wu, C.; Wang, R. *Polym. Adv. Technol.* **2012**, *23*, 1429.
22. Wu, H.; Zheng, B.; Zheng, X.; Wang, J.; Yuan, W.; Jiang, Z. *J. Power Sources* **2007**, *173*, 842.
23. Montiel, V.; Saez, A.; Expósito, E.; García-García, V.; Aldaz, A. *Electrochem. Commun.* **2010**, *12*, 118.
24. Casado, C.; Ambroj, D.; Mayoral, Á.; Vispe, E.; Téllez, C.; Coronas, J. *Eur. J. Inorg. Chem.* **2011**, *2011*, 2247.
25. Rubio, C.; Murillo, B.; Casado-Coterillo, C.; Mayoral, A.; Téllez, C.; Coronas, J.; Berenguer-Murcia, Á.; Cazorla-Amorós, D. *Int. J. Hydrogen Energy* **2014**, *39*, 13180.
26. Del Castillo, A.; Alvarez-Guerra, M.; Irabien, A. *AIChE J.* **2014**, *60*, 3557.
27. Casado-Coterillo, C.; López-Guerrero, M. d. M.; Irabien, A. *Membranes* **2014**, *4*, 287.
28. Pérez-Carvajal, J.; Lalueza, P.; Casado, C.; Téllez, C.; Coronas, J. *Appl. Clay Sci.* **2012**, *56*, 30.
29. Neves, L. A.; Benavente, J.; Coelho, I. M.; Crespo, J. G. *J. Membr. Sci.* **2010**, *347*, 42.
30. White, J. D.; Cussler, E. L. *J. Membr. Sci.* **2006**, *278*, 225.
31. Zhao, J.; Wang, F.; Pan, F.; Zhang, M.; Yang, X.; Li, P.; Jiang, Z.; Zhang, P.; Cao, X.; Wang, B. *J. Membr. Sci.* **2013**, *446*, 395.
32. Liu, C.; Bai, R. *J. Membr. Sci.* **2006**, *284*, 313.
33. Dambies, L.; Guimon, C.; Yiacoumi, S.; Guibal, E. *Coll. Surf. A* **2001**, *177*, 203.
34. de Godoi, F. C.; Rodriguez-Castellon, E.; Guibal, E.; Beppu, M. M. *Chem. Eng. J.* **2013**, *234*, 423.
35. Wan, Y.; Peppley, B.; Creber, K. A. M.; Bui, V. T. *J. Power Sources* **2010**, *195*, 3785.
36. Wu, Y.; Wu, C.; Xu, T.; Fu, Y. *J. Membr. Sci.* **2009**, *329*, 236.
37. Lin, Z.; Rocha, J.; Valente, A. *Chem. Commun.* **1999**, *1999*, 2489.
38. Xiong, Y.; Liu, Q. L.; Zhang, Q. G.; Zhu, A. M. *J. Power Sources* **2008**, *183*, 447.
39. Lin, B.; Dong, H.; Li, Y.; Si, Z.; Gu, F.; Yan, F. *Chem. Mater.* **2013**, *25*, 1858.
40. Pauliukaite, R.; Ghica, M. E.; Fatibello-Filho, O.; Brett, C. M. A. *Anal. Chem.* **2009**, *81*, 5364.
41. Mohammad, S.; Niya, R.; Hoofar, M. *J. Power Sources* **2013**, *240*, 281.
42. Yun, S.-H.; Shin, S.-H.; Lee, J.-Y.; Seo, S.-J.; Oh, S.-H.; Choi, Y.-W.; Moon, S.-H. *J. Membr. Sci.* **2012**, *417-418*, 210.
43. Asghari, S.; Mokmeli, A.; Samavati, M. *Int. J. Hydrogen Energ.* **2010**, *35*, 9283.
44. Chávez, E. L.; Oviedo-Roa, R.; Contreras-Pérez, G.; Martínez-Magadán, J. M.; Castillo-Alvarado, F. L. *Int. J. Hydrogen Energy* **2010**, *35*, 12141.
45. Wan, Y.; Peppley, B.; Creber, K. A. M.; Bui, V. T.; Halliop, E. *J. Power Sources* **2006**, *162*, 105.
46. Xiong, Y.; Wang, H.; Wu, C.; Wang, R.-M. *Polym. Adv. Technol.* **2011**, *23*, 1429.
47. Singh, P. K.; Bhattacharya, B.; Nagarale, R. K.; Kim, K. M.; Rhee, H.-W. *Synth. Met.* **2010**, *160*, 139.
48. Matsuoka, K.; Iriyama, Y.; Abe, T.; Matsuoka, M.; Ogumi, Z. *J. Power Sources* **2005**, *150*, 27.
49. Won, W.; Feng, X.; Lawless, D. *J. Membr. Sci.* **2002**, *209*, 493.